Solution of the Dirac equation for hydrogenlike systems exposed to intense electromagnetic pulses

Sølve Selstø,* Eva Lindroth, and Jakob Bengtsson

Atomic Physics, Fysikum, AlbaNova University Center, Stockholm University, SE-106 91 Stockholm, Sweden

The time-dependent Dirac equation is solved numerically and compared to the corresponding prediction of the nonrelativistic Schrödinger equation for hydrogenlike systems exposed to intense laser pulses. It is found that for a correct description of effects beyond the dipole approximation, virtual electron-positron pairs can be very important. Relativistic effects in the ionization dynamics of highly charged systems are studied.

PACS number(s): 42.50.Hz, 31.30.jc, 32.80.Fb, 33.20.Xx

I. INTRODUCTION

With the ongoing improvements in laser technologies, intensities are reached that make it important to test the common nonrelativistic approaches for light-matter interaction against a full relativistic treatment based on the Dirac equation. In addition, the higher photon energies, envisaged with the upcoming free-electron laser projects, will most probably result in measurements on ions and then also the requirement on the atomic structure description will call for a relativistic treatment of the ion laser-pulse interaction. In spite of the current large theoretical interest in the interaction of intense short electromagnetic pulses with atoms, the relativistic equations tend to be treated in a simplified manner, e.g., by adapting a classical description [1] or by resorting to lower dimensional [2–5] approaches. A recent review of the field can be found in Ref. [6]. Here we present a full solution of the time-dependent Dirac equation for hydrogenlike ions initially prepared in the ground state and subjected to short electromagnetic pulses.

An important issue when the Dirac equation is treated is the handling of its negative energy solutions. Dirac's original prescription was to consider the negative energy states to be populated even in vacuum. The Pauli principle forces then additional particles to occupy positive energy states. This prescription is kept by quantum electrodynamics, but the interpretation is slightly rephrased. An unoccupied negative energy state represents now the presence of a positron and annihilation is the physical manifestation of the transition of an electron to such an empty state. Due to the possibility of annihilation and its time reverse, pair creation, the number of particles is no longer constant in time. Still, a new electron-positron pair cannot be created if not an energy amount equivalent to at least twice the electron rest mass energy is available and one might therefore think that the process of pair creation can be neglected under normal conditions. However, there is always the possibility for creation and subsequent annihilation of *virtual* electron-positron pairs. In a practical calculation this is accounted for by the admixture of negative energy states into the electron wave function, see e.g., the discussion by Furry [7]. It was noted already by

Dirac [8] that these effects can be very important: "for a free electron and radiation of low frequency, where the classical formula holds, the whole of the scattering comes from such intermediate states." The phenomenon is discussed in more detail by Sakurai [9] in connection with Thomson scattering: "…it is absolutely necessary to take into account transitions involving negative energy states if we are to obtain the correct non-relativistic results." Yet, this is still today not always recognized. We show below that virtual electron-positron pairs greatly influence the interaction with a time-varying electromagnetic field beyond the so-called dipole approximation when the interaction with the electromagnetic field is described in the velocity gauge.

In this study we treat hydrogenlike ions. We use complex rotation and investigate the probability for the systems to remain in the ground state, as well as the ionization rate during exposure to a short electromagnetic pulse. The theory behind the calculation is recapitulated in Sec. II. The method is described in Sec. III and finally the results are presented and discussed in Sec. IV.

II. THEORY

We will follow the time evolution as governed by the time-dependent Dirac equation;

$$i\hbar\frac{\partial}{\partial t}\Psi = H_D\Psi, \tag{1}$$

where

$$H_D = \{c\boldsymbol{\alpha}\cdot[\mathbf{p}+e\mathbf{A}(\eta)]+V+mc^2\beta\},$$

$$\boldsymbol{\alpha}\equiv\begin{pmatrix}0 & \boldsymbol{\sigma}\\ \boldsymbol{\sigma} & 0\end{pmatrix}, \quad \beta\equiv\begin{pmatrix}I_2 & 0\\ 0 & -I_2\end{pmatrix}, \tag{2}$$

where I_2 is a 2×2 unity matrix and the Lorenz invariant quantity η is defined as

$$\eta \equiv k_\mu x^\mu = \omega t - \mathbf{k}\cdot\mathbf{r}. \tag{3}$$

$\mathbf{A}$ is the vector potential such that $\mathbf{E}=-\partial\mathbf{A}/\partial t$ and $\mathbf{B}=\nabla\times\mathbf{A}$. We will work in the Coulomb gauge and $\mathbf{A}$ is thus perpendicular to the wave vector of the electromagnetic field $\mathbf{k}$. Since the Dirac matrices $\boldsymbol{\alpha}$ and β are 4×4 matrices, also the wave function in Eq. (1) will have four components. The

*Present address: Centre of Mathematics for Applications, University of Oslo, N-0316 Oslo, Norway.

spatial part of it will have two components, often called the large and small component, respectively. This refers to the fact that for electrons that travel with nonrelativistic velocities the contribution from the *large* component to the probability density is $\sim 1/\alpha^2$ larger than those from the *small* component, where α is the fine structure constant.

Equation (2) is given in what is often called the *velocity form*. Compared to its nonrelativistic counterpart,

$$i\hbar \frac{\partial \Psi^{\text{NR}}}{\partial t} = \left[\frac{\mathbf{p}^2}{2m} + V + \frac{e}{m}\mathbf{A}(\eta)\cdot\mathbf{p} + \frac{e^2}{2m}\mathbf{A}^2(\eta) \right]\Psi^{\text{NR}}, \quad (4)$$

it has a compact structure. While Eq. (4) has one term linear and one term quadratic in the vector potential, the relativistic equation, Eq. (2), has only a linear term, through which the vector potential couples to the Dirac $\boldsymbol{\alpha}$ matrix and thus to the electron spin. Important for the findings presented below is the fact that the interaction is nondiagonal with respect to the large and small component of the relativistic wave function. We will return to this point later. If the spatial variations of $\mathbf{A}$ are neglected, only the electric component of the field can be represented and we get the *dipole* approximation. The effects accounted for within this approximation dominate the physics for a wide range of intensities and frequencies. The main interest here is, however, effects that are beyond a nonrelativistic treatment in the dipole approximation. When such effects are accounted for through a refined treatment of the nonrelativistic Schrödinger equation, Eq. (4), it is customary to distinguish between relativistic corrections and the corrections that can be accounted for through a space-dependent vector potential (i.e., magnetic effects, electric quadrupole effects etc.). For strong time-dependent electromagnetic fields it is well known [10–12] that the dominating contribution of the latter kind comes from the so-called diamagnetic term, $\sim \mathbf{A}^2$, in Eq. (4). Physically, the dominating effect is due to the coupling of a fast electron, accelerated by the electric component of the time varying field, with the magnetic component of the same field. Relativistic corrections, on the other hand, are expected when the ponderomotive energy ($|e\mathbf{E}_0|^2/4m\omega^2$) approaches a substantial fraction of the mass energy (mc^2). To account for such effects within the framework of Eq. (4) one could for example make a Foldy-Wouthuysen [13] type transformation of Eq. (2), which will lead to the nonrelativistic equation with the usual Breit-Pauli corrections plus additional terms depending on the external field. If, instead, we choose to work directly with the Dirac equation, the dipole approximation is still obtained if the space variations of the vector potential are neglected, but there is no easy way to distinguish between diamagnetic corrections and other corrections to it, and the relativistic effects are now always present.

A. Dynamics and negative energy states

The question of how the negative energy eigenstates to the Dirac Hamiltonian (2) should be treated is still today giving rise to discussions. For example, Ref. [14], which presents a fully relativistic close-coupling method for electron collisions with atoms and ions, argues that negative energy eigenstates of the unperturbed Hamiltonian H_0 should

be removed from the basis as long as the creation of real positron-electron pairs (in the scattering process) is energetically out of reach. The argumentation refers to Dirac's original statement that the negative energy continuum is filled. The conclusion reached in the present study is actually very different. We find that, since the negative energy continuum of the full, time-dependent Hamiltonian $H(t)$ and the unperturbed one, H_0, differ, exclusion of negative energy eigenstates of H_0 leads to inclusion of negative energy eigenstates of the actual Hamiltonian $H(t)$.

It is constructive to start to look at the problem from a mathematical point of view. A trivial but still very important observation is then that only together do the negative ($E < -mc^2$) and positive eigenenergy states of Hamiltonian (2) form a complete set. The distinction between negative and positive energy states (positron and electron states) is further not fixed, but changes with the field present [15]. If we for example want to express the ground state of hydrogen in a basis of hydrogenlike functions for *any* other charge than unity, we need to allow also for negative energy eigenstates of that Hamiltonian. Mathematically this is just a consequence of the completeness of the full set of solutions, but not of the positive energy solutions alone. Physically we can understand that all states are altered when the external field changes and thus that the Pauli blockade resulting from the "filled negative energy sea" changes as well. Formally the adjustment of the negative energy states (empty positron states) is accomplished through the creation of virtual electron-positron pairs, which in turn provides the possibility for electron-positron annihilation, i.e., the transitions of electrons into negative energy states.

Is the situation any different when we deal with a time-dependent field? As long as we deal with a field much smaller than the critical field needed for a substantial amount of real pair production, $E_{\text{crit}} = m^2c^3/e\hbar \approx 1.3 \times 10^{18}$ V/m $\approx 3 \times 10^6$ a.u. [16], we do not think so. The definition of positive and negative energy states changes now at every instance in time, and in our opinion the blockade imposed from the "filled negative energy sea" changes consequently. Support for this view can be obtained from early studies of relativistic scattering theory [7]. Another supporting finding was reported recently by Boca and Florescu [5]. Studying a one-dimensional model atom exposed to an electromagnetic pulse, they found that negative energy states of the field free Hamiltonian may indeed be significantly populated during the pulse, even when the ponderomotive energy of the electron was two orders of magnitude smaller than its rest mass energy, whereas such states belonging to a basis of field dressed states remain virtually unpopulated.

Still one might ask how large the effects from virtual electron-positron pair creation can be. In the example above where the hydrogen ground state is expanded in a basis set of eigenstates of the Hamiltonian for a hydrogenlike ion, these effects will be small and they will vanish in the nonrelativistic limit. Here the situation is very different. It will be demonstrated below, Sec. IV A, that if we neglect electron-positron pair creation and annihilation, while sticking to the definition of them given by the zero-field Hamiltonian, we no longer get correct results in the nonrelativistic limit.

In order to illustrate the effects of different choices when the negative energy states are excluded from the calculation

we compare in Sec. IV A results obtained following two rea-sonings. In the first case we simply remove all eigenstates of H_0 that have an energy less than $-mc^2$ before propagation. In the second case we diagonalize the full, time-dependent Hamiltonian $H(t)$. The negative eigenenergies of this Hamil-tonian are consecutively removed from the basis. Hence, in the latter method diagonalization is necessary at every time step, and the Hilbert space at hand changes in time.

III. METHOD

The solution of the Dirac equation is based on the method by Salomonson and Öster, Ref. [17], where a one-particle Dirac Hamiltonian is discretized in a spherical box and on an exponential radial mesh, $r_i = e^{x_i}$. Diagonalization of the re-sulting matrix gives a finite radial basis set for each angular symmetry (defined by ℓ, j, and in principle also by m_j), which is complete on the chosen grid. Keeping angular sym-metries up to some maximum ℓ and j, we have a basis set that can be used to solve the time-dependent Eq. (1). The basis set may refer either to the Dirac Hamiltonian without the time-varying field or to the full Hamiltonian (including the time-varying field) at a particular instance in time. Both approaches have been used and they lead naturally to tech-nically rather different solutions of the time-dependent equa-tion as will be discussed below. If the basis set refers to the full Hamiltonian, it can be obtained either through a direct diagonalization or through a stepwise procedure where the first step gives the basis set with respect to it without the time-varying field. In the second step this basis set is used to diagonalize the full Hamiltonian. If no truncations of basis sets are made, these two methods are equivalent, in principle as well as in practice.

We have further imposed uniform complex rotation—defined by $\mathbf{r} \rightarrow \mathbf{r}e^{i\theta}$—for all the calculations presented here. This has not been stated explicitly in the equations, but the scaling with a complex phase should be considered as im-plicit whenever the radial variable is referred to. The grid discretization of the Dirac Hamiltonian [17] and complex rotation has been combined earlier in a different context; see Ref. [18] and references therein. The complex rotation has here two important advantages. First, it ensures that the con-tinuum can be covered by very few basis states within each symmetry. Second, the transformation tends to "kill off" high energy components of the wave function so that the rotated wave function is described more easily than the true unro-tated one on a finite grid [19]. The population of bound states is, in principle, unchanged by the rotation, whereas informa-tion about the ionized part of the system may be hard to extract from the rotated wave function. Hence, this is an ideal method for calculations of excitation and ionization probabilities. One might be skeptical, though, to the use of complex rotation in connection with functions that are peri-odic in space, since such a function diverges exponentially after rotation. This would indeed be a problem for a plane-wave vector potential extending over the whole space, but for an electromagnetic pulse the situation is much better since the envelope kills the interaction in far off regions. For instance, for a pulse with a Gaussian envelope we have

$$
\begin{aligned}
A \sim {}& \exp[-(\eta - \eta_0)^2/2\sigma^2]\cos\,\eta \rightarrow e^{i\,\mathrm{Im}[-(\eta - \eta_0)^2/2\sigma^2]} \\
& \times e^{-[(\omega t - \eta_0)^2 + (kx)^2\cos(2\theta) - 2(\omega t - \eta_0)kx\cos\theta]/2\sigma^2} \\
& \times \frac{1}{2}[e^{i\,\mathrm{Re}(\eta)}e^{+kx\sin\theta} + e^{-i\,\mathrm{Re}(\eta)}e^{-kx\sin\theta}].
\end{aligned}
\tag{5}
$$

It is seen that as $|x|$ approaches infinity, the divergences in the exponential factors in the carrier are "killed off" by the term proportional to x^2 in the exponential of the envelope provided that $|\theta| < 45°$.

The atomic system is initially prepared in the ground state. In Sec. III A we describe how the calculation of the coupling to the electromagnetic field, causing excitation and ionization, is done in practice.

A. Coupling to the electromagnetic field

The stationary solutions to the time-independent Dirac equation, i.e., the eigenstates of Hamiltonian (2) with $\mathbf{A}=\mathbf{0}$, for an electron in a spherically symmetric time-independent potential may be written as

$$
\psi_{n,\kappa,j,m}(\mathbf{r}) = \frac{1}{r}\begin{pmatrix} P_{n,\kappa}(r)X_{\kappa,j,m} \\ iQ_{n,\kappa}(r)X_{-\kappa,j,m} \end{pmatrix},
\tag{6}
$$

where

$$
\kappa \equiv \begin{cases} l, & j = l - 1/2 \\ -(l+1), & j = l + 1/2, \end{cases}
$$

and

$$
X_{\kappa,j,m} \equiv \sum_{m_l,m_s} \langle l_\kappa, m_\kappa, s = 1/2, m_s | j, m\rangle Y_{l_\kappa,m_l}(\hat{\mathbf{r}})\chi_{m_s},
\tag{7}
$$

i.e., the spinors $X_{\kappa,j,m}$ are linear combinations of products of spherical harmonics and spin eigenstates.

The vector potential $\mathbf{A}$ in the interaction term in Eq. (2), $ec\boldsymbol{\alpha}\cdot\mathbf{A}$, is chosen to have the form

$$
\mathbf{A}(\eta) = \begin{cases} \dfrac{\mathbf{E}_0}{\omega}\sin^2\left(\dfrac{\pi\eta}{\omega T}\right)\cos(\eta + \varphi), & \eta \in [0, T\omega] \\ \mathbf{0}, & \text{otherwise}, \end{cases}
\tag{8}
$$

with η defined in Eq. (3) and $A_0 = E_0/\omega$. The dipole approxi-mation, in which the spatial dependence of the field is ne-glected, is obtained by the substitution $\eta \rightarrow \omega t$. Within this approximation with polarization along the z axis the quantum number m remains a good quantum number also in the pres-ence of the field. This simplifies the numerical scheme con-siderably. In this context, the couplings read

$$
\langle \psi_{n',\kappa',j',m} | ec\boldsymbol{\alpha}\cdot\mathbf{A} | \psi_{n,\kappa,j,m}\rangle
$$

$$
\begin{aligned}
= -iecA(t)\Bigg(& \int_0^\infty Q_{n',\kappa'}P_{n,\kappa}\,dr\langle X_{-\kappa',j',m} | \sigma_z | X_{\kappa,j,m}\rangle \\
& - \int_0^\infty P_{n',\kappa'}Q_{n,\kappa}\,dr\langle X_{\kappa',j',m} | \sigma_z | X_{-\kappa,j,m}\rangle \Bigg),
\end{aligned}
\tag{9}
$$

with angular factors

$$\langle X_{\kappa',j',m}|\sigma_z|X_{\kappa,j,m}\rangle = (-1)^{j'-j+l_\kappa-m+s}(2j'+1)(2j+1)(s\|\boldsymbol{\sigma}\|s)$$

$$\times \delta_{l_{\kappa'},l_\kappa} \begin{Bmatrix} s & j' & l_\kappa \\ j & s & 1 \end{Bmatrix}$$

$$\times \begin{pmatrix} j & 1 & j' \\ m & 0 & -m \end{pmatrix}\bigg|_{s=1/2}, \tag{10}$$

where the reduced matrix element $(s\|\boldsymbol{\sigma}\|s)|_{s=1/2}=\sqrt{6}$.

To go beyond the dipole approximation the full spatial dependence of the vector potential, Eq. (8), is needed. One possibility is to expand the vector potential in plane waves of the type $\exp[\pm i(\Omega t - \mathbf{K}\cdot\mathbf{r})]$. The spatial part may be further expanded in spherical harmonics,

$$\exp(\pm i\mathbf{K}\cdot\mathbf{r}) = 4\pi\sum_{\lambda,\mu}(\pm i)^\lambda j_\lambda(Kr)Y^*_{\lambda,\mu}(\hat{\mathbf{k}})Y_{\lambda,\mu}(\hat{\mathbf{r}}), \tag{11}$$

where $j_\lambda(Kr)$ is a spherical Bessel function of the first kind. Hence, the total coupling, $ec\boldsymbol{\alpha}\cdot\mathbf{A}$, may be calculated as a sum of couplings of the type $j_\lambda(Kr)Y_{\lambda,\mu}(\hat{\mathbf{r}})\alpha_q$. The index $q = \pm 1, 0$ corresponds to the polarization direction. Specifically,

$$\langle\psi_{n',\kappa',j',m'}|j_\lambda(Kr)Y_{\lambda,\mu}(\hat{\mathbf{r}})\alpha_q|\psi_{n,\kappa,j,m}\rangle$$

$$= -i\Bigg(\int_0^\infty Q_{n',\kappa'}j_\lambda P_{n,\kappa}dr\langle X_{-\kappa',j',m'}|Y_{\lambda,\mu}\sigma_q|X_{\kappa,j,m}\rangle$$

$$- \int_0^\infty P_{n',\kappa'}j_\lambda Q_{n,\kappa}dr\langle X_{\kappa',j',m'}|Y_{\lambda,\mu}\sigma_q|X_{-\kappa,j,m}\rangle\Bigg). \tag{12}$$

Numerical values for the spherical Bessel functions of complex arguments are obtained by a combination of an analytical expression valid for small $|kr|$ [20] and a numerical routine provided in Ref. [21]. By combining the spherical tensor operators $C^\lambda_\mu \equiv \sqrt{4\pi/(2\lambda+1)}Y_{\lambda,\mu}$ and the spin operator σ_q,

$$C^\lambda_\mu\sigma_q = \sum_{L=\lambda-1}^{\lambda+1}\langle\lambda,\mu,1,q|L,M\rangle\{\mathbf{C}^\lambda\cdot\boldsymbol{\sigma}\}^L_M, \quad M = \mu+q, \tag{13}$$

the angular parts of the full coupling, Eq. (12), may be written

$$\langle X_{\kappa',j',m'}|\{\mathbf{C}^\lambda\cdot\boldsymbol{\sigma}\}^L_M|X_{\kappa,j,m}\rangle$$

$$= (-1)^{2j-j'-m'}\sqrt{(2L+1)(2j+1)(2j'+1)}$$

$$\times (l_{\kappa'}\|\mathbf{C}^\lambda\|l_\kappa)(s\|\boldsymbol{\sigma}\|s)\begin{Bmatrix} l_{\kappa'} & \lambda & l_\kappa \\ j' & L & j \\ s & 1 & s \end{Bmatrix}$$

$$\times \begin{pmatrix} L & j & j' \\ M & m & -m' \end{pmatrix}\bigg|_{s=1/2}. \tag{14}$$

We have thus obtained a multipole expansion of the interaction with the vector potential expressed as a plane wave. The different terms in the expansion can be classified according to their angular structure in Eq. (14). The electric dipole type interaction is for example obtained with $\lambda = 0$ and $L = 1$. If the

electric field is polarized in the z direction, we have in addition $M = 0$ leading to the selection rule, $m = m'$, as discussed above. Magnetic dipole type interactions are obtained with $\lambda = 1$ and $L = 1$, etc. If instead all possible interactions leading to a transition from $|\kappa\ell j\rangle$ to $|\kappa'\ell'j'\rangle$ are included, there are no longer any restrictions on which m state that can be populated. Hence, in such a treatment, the number of required basis states is proportional to $2(\ell_{\max}+1)^2$ as opposed to $2\ell_{\max}+1$ in the dipole case [with $j_{\max}=\ell_{\max}+1/2$]. It is thus clear that a substantial increase in computational effort is required to consider all types of interactions. In addition the evaluation of the couplings becomes more cumbersome. Note finally that a Fourier expansion of the vector potential describing an electromagnetic *pulse* as in Eq. (8) requires infinitely many plane-wave terms and it is thus necessary to resort to approximations. We will return to this issue in Sec. III C.

B. Nonrelativistic treatment

In order to distinguish truly relativistic effects from higher order multipole terms, cf. Eqs. (12)–(14), predictions from the Dirac equation, Eq. (1), must be compared with those from the Schrödinger equation, Eq. (4). As was mentioned above it has previously been demonstrated that in the high intensity regime, the contributions beyond the dipole approximation come more or less exclusively from the diamagnetic term [10–12], $\sim\mathbf{A}^2$, in the Schrödinger Hamiltonian, Eq. (4). Hence, for simplicity, we include in our nonrelativistic calculation such contributions from this term only. If we again use the expansion in plane waves and utilize Eq. (11), we find

$$\langle\psi^{\mathrm{NR}}_{n',l',m'}|e^{\pm i\mathbf{K}\cdot\mathbf{r}}|\psi^{\mathrm{NR}}_{n,l,m}\rangle$$

$$= (-1)^{m'}\sqrt{4\pi(2l'+1)(2l+1)}\sum_{\lambda=1}^{l_{\max}}i^{\pm\lambda}\begin{pmatrix} l' & \lambda & l \\ 0 & 0 & 0 \end{pmatrix}$$

$$\times \int R_{n',l'}(r)j_\lambda(Kr)R_{n,l}(r)dr$$

$$\times \sum_{\mu=-\lambda}^\lambda Y^*_{\lambda,\mu}(\hat{\mathbf{k}})\begin{pmatrix} l' & \lambda & l \\ -m' & \mu & m \end{pmatrix}, \tag{15}$$

where $\psi_{n,l,m}(\mathbf{r})=1/rR_{n,l}(r)Y_{l,m}(\hat{\mathbf{r}})$ are eigenstates to the unperturbed Hamiltonian. Alternatively, corrections to the dipole approximation may be found by expanding the interaction to first order in the spatial coordinate of propagation, say x [10,22]:

$$\frac{e^2}{2m}[A(\eta)]^2 \approx \frac{e^2}{2m}\Bigg\{[A(\omega t)]^2 - \frac{x\omega}{c}\Bigg[2A(\eta)\frac{dA(\eta)}{d\eta}\Bigg]_{x=0}\Bigg\}. \tag{16}$$

The couplings induced by x are then found as

$$\langle \psi^{\mathrm{NR}}_{n',l',m'}|x|\psi^{\mathrm{NR}}_{n,l,m}\rangle = \frac{(-1)^{l'-m'}}{\sqrt{2}}\int R_{n',l'}rR_{n,l}dr(l'\|\mathbf{C}^1\|l)$$
$$\times\left[\begin{pmatrix} l' & 1 & l \\ -m' & -1 & m \end{pmatrix} - \begin{pmatrix} l' & 1 & l \\ -m' & 1 & m \end{pmatrix}\right].$$
$$(17)$$

For simplicity we have used the last procedure for the comparisons below.

C. How to incorporate nondipole effects

We will now return to the question of how the full interaction can be implemented in our propagation scheme. Obviously, when using a time-independent basis representation for the wave function, be it eigenstates to some time-independent Hamiltonian or simply grid points in time, the spatial dependence and the time dependence of the interaction should preferably be separated to avoid calculations of new couplings at every time step. We would thus like to write the time-dependent interaction term

$$H'(t,\mathbf{r}) = ce\boldsymbol{\alpha}\cdot\mathbf{A}(\eta) \qquad (18)$$

as

$$H'(t,\mathbf{r}) = \sum_n c_n H_n^t(t)H_n^r(\mathbf{r}). \qquad (19)$$

Taylor or Fourier expansions are natural ways to achieve such a separation.

For a pulse with high central frequency ω and a duration T that extends over several optical cycles, the carrier depends more strongly on the spatial coordinate than the envelope does. It may thus seem like a good approximation to neglect the spatial dependence in the envelope and retain it only in the carrier;

$$A(\eta) \approx \frac{E_0}{\omega}\sin^2(\pi t/T)\cos(\eta+\varphi). \qquad (20)$$

In this case the interaction may be written

$$H' \approx \frac{ce}{2\omega}\boldsymbol{\alpha}\cdot\mathbf{E}_0\sin^2(\pi t/T)\times(e^{-i(\omega t+\varphi)}e^{i\mathbf{k}\cdot\mathbf{r}}+e^{i(\omega t+\varphi)}e^{-i\mathbf{k}\cdot\mathbf{r}}).$$
$$(21)$$

Note that numerical problems may arise when combining Eq. (21) with complex rotation. The reason is that the interaction is no longer confined in space (there is no spatial dependence in the envelope), and for large distances the space periodic function will diverge. In practice this imposes an upper limit to the applied rotation angle θ. Another more fundamental problem arising from Eq. (20) is that since the vector potential $\mathbf{A}$ no longer depends only on the Lorenz invariant quantity η, the Lorenz covariance of the Dirac equation is lost. The approximation in Eq. (21) is here used in connection with the calculation of ionization rates in Sec. IV B below. It is only meaningful to talk about a rate during a period in time when the field amplitude is constant. Thus, if it makes sense to calculate a rate, the approximation to neglect the

spatial dependence in the envelope is automatically justified.

As mentioned in Sec. III A, a more general method to obtain the interaction on the form given in Eq. (18) would be to make a full Fourier expansion of the interaction,

$$H' = \frac{ce}{\omega}\boldsymbol{\alpha}\cdot\mathbf{E}_0\sum_n c_n\exp\left(i\frac{2\pi n}{P}\eta\right), \qquad (22)$$

where the expansion coefficients c_n are found from the field. Since, in a real calculation, the Fourier expansion has to be truncated, we will never obtain a true pulse but rather a train of pulses. P determines the fundamental period of the Fourier terms and at a first glance it may seem natural to choose it such that it corresponds to the length of the pulse, $P=\omega T$. T is here the pulse length and equals an integer number, N, of cycles of the carrier wave, $T=N2\pi/\omega$. With $P=\omega T$ the envelope in the vector potential, Eq. (8), can be written exactly with three Fourier terms and then the whole vector potential requires only six terms with $n=\pm N$, $\pm(N\pm 1)$. In order to interact with one pulse only, the time propagation should now be made from $t=0$ to $t=T$ only. However, as the atom gains spatial extension during the interaction, the true interaction time is in fact slightly longer than T. Now a problem arises; if a longer propagation time is used then the next (and nonphysical) pulse of the "pulse train" might interfere with the dynamics. In principle this problem can be solved by keeping enough terms in the Fourier expansion that there is a clear dead time between the pulses so that the physical pulse has time to leave the interaction region before the next pulse enters it. We would thus like the pulse train to have a periodicity longer than T, or equivalently we would like to use $P>\omega T$. The drawback now is that with such a choice the vector potential can no longer be expressed with a finite number of Fourier terms, and for a reasonable representation of, e.g., a pulse of five optical cycles at least 20 terms are needed. In reality the effect we miss if the interaction time is not increased is rather small. This can be understood from the fact that the drift of the electron, caused by the electric field, is of the order of a few Bohr radii for the fields studied here, and thus the needed increase in interaction time is around 1/137 a.u. In view of the complexity of the just discussed improved scheme and also of the fact that the spatial extension in the direction of the pulse is very small, the present calculation is made with $P=\omega T$ and is propagated until $t=T$. The reason that the spatial extension in the propagation direction is very small is that it is driven by the magnetic field, while the electric field drives the electron in a direction perpendicular to the propagation direction.

From this consideration we expect that the introduced error in the final wave function should be of minor importance. Still, for high intensities and short pulses, it can be challenging to find the correct ionization probability since the population of Rydberg states may be somewhat modified by the fact that the Hamiltonian at the time T does not completely coincide with the unperturbed one. The predicted population of the ground state, which is well localized, should, however, not suffer from this problem.

D. Time propagation

Two different schemes have been used to solve the time-dependent Dirac (or Schrödinger) equation. In the first scheme the wave function is expanded in eigenstates, Φ^0, to the time-independent Hamiltonian, H_0,

$$\Psi(t) = \sum_k c_n(t) \Phi_k^0. \tag{23}$$

Equation (1) is now transformed to an equation for the c coefficients, which in matrix form reads

$$\dot{\mathbf{c}} = -\frac{i}{\hbar} \left[\mathbb{H}_0 + \sum_{r=1}^{R} f_r(t) \mathbb{H}'_r \right] \mathbf{c}, \tag{24}$$

where $\mathbb{H}_n^{(')}$ are matrices and $\mathbf{c}(t)$ is a vector containing the expansion coefficients of the wave function. The number of terms in the perturbation, R, is one in the dipole approximation, two for Eq. (21) as well as for the nonrelativistic approximate account of effects beyond the dipole approximation, Eq. (16), and six for the pulse train approach described in connection with Eq. (22). Equation (24) has been solved with an adaptive step Runge-Kutta method, which has the advantage that the results it provides are "always" accurate. The downside of this method is that it may be slow when energies, i.e., diagonal elements of $\mathbb{H}_0$, with large absolute values are involved. With this scheme it is hard to avoid inclusion of negative energy states to $H(t)$, but it is straightforward to remove negative energy states with respect to H_0—it is just to omit them from expansion (23). In fact inclusion of negative energy states to H_0 is here hard to combine with complex rotation since the energies of such states have positive imaginary parts, which would cause the wave function to blow up when propagated.

In contrast, truncation of negative energy states of the perturbed Hamiltonian $H(t)$ is readily done with our second approach to the time propagation. We work then directly with the propagator

$$\Psi(t + \Delta t) \approx e^{-iH(t)\Delta t/\hbar} \Psi(t) \tag{25}$$

and utilize the *field dressed* eigenstates $\Phi_j(t)$, with eigenvalues $E_j(t)$, of the full Hamiltonian at a specific time, $H(t)$, to express the exponentiation of the Hamiltonian,

$$e^{-iH(t)\Delta t/\hbar} = \sum_j e^{-iE_j\Delta t/\hbar} |\Phi_j(t)\rangle\langle\Phi_j(t)|. \tag{26}$$

Diagonalization of $H(t)$ to obtain the set Φ_j is here done at every time step; see Ref. [19] for further details. Negative energy states of $H(t)$ can now be excluded just by adjusting the sum in Eq. (26). An important point here is that, although negative energy states of the full Hamiltonian are excluded, it allows a certain admixture of negative energy states of H_0. As the method relies on Eq. (25), convergence in Δt must be checked carefully and naturally the method quickly becomes very costly when large basis sets are at hand. Therefore it is crucial to keep the number of basis states low, but still adequate. To this end, complex rotation is very useful.

When the second approach is combined with complex rotation numerical problems might arise since there is a possibility for the magnitude of the (rotated) wave function to
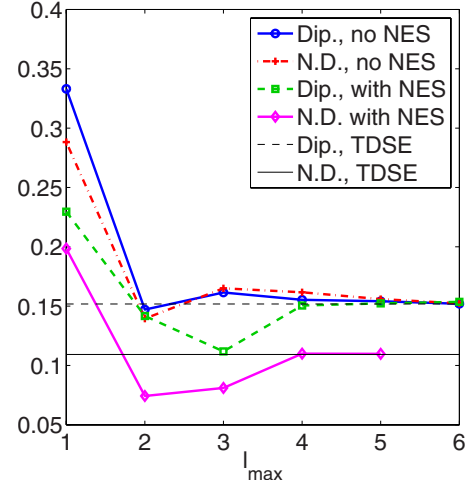

FIG. 1. (Color online) The convergence with respect to ℓ_{max} of the probability to remain in the initial state (the ground state) for a hydrogen atom exposed to a laser pulse of a maximum electric field strength $E_0 = 30$ a.u. ($\sim 3.16 \times 10^{19}$ W/cm^2), a central frequency $\omega = 2$ a.u. (corresponding to a photon energy of 54.4 eV) and a duration of five optical cycles (corresponding to 380 as). For the relativistic calculations four different approaches have been applied. Specifically, calculations have been performed with and without the dipole approximation ("Dip./N.D.") and both including and excluding negative energy states ("NES") of the unperturbed Hamiltonian. The ℓ_{max}-converged nonrelativistic results ("TDSE") have also been included as lines for comparison (thin black curves).

increase over certain time periods. This behavior can be traced back to the anti-Hermitian part of the scaled interaction as noted in [23] and discussed in [19]. The problems arise if the magnitude blow up beyond what is numerically stable, which might happen if θ is chosen too large. Hence, the rotation angle must be chosen increasingly moderate as the intensity of the field increases—at the expense of having to include more radial points in the grid.

IV. RESULTS AND DISCUSSION

A. Negative energy states and nondipole effects

In Fig. 1 we show the convergence of the probability for a hydrogen atom to remain in the ground state after being exposed to an electromagnetic pulse with central frequency $\omega = 2.0$ a.u., which corresponds to a photon energy of 54.4 eV, a peak electric field strength $E_0 = 30$ a.u., corresponding to a peak intensity of 3.16×10^{19} W/cm^2, and a pulse duration T that corresponds to $N = 5$ optical cycles (~ 380 as). It is known from calculations performed in the Kramers-Henneberger frame that effects beyond the dipole approximation are significant for such a pulse [22], but since the ponderomotive energy is only $\sim 0.3\%$ of the electron rest mass energy, relativistic effects are expected to be small. Hence comparison with the time-dependent Schrödinger equation seems reasonable. The relativistic survival probability of the ground state is calculated with two different implementations of the field: the dipole approximation and the pulse train implementation discussed in connection with Eq.
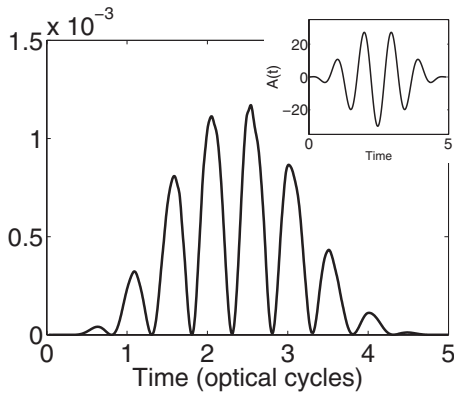
FIG. 2. The population of negative energy states of the unperturbed Hamiltonian H_0 during the electromagnetic pulse for the same case as in Fig. 1. Although this quantity depends on the rotation angle θ, which is $10°$ here, it demonstrates that population of such states is significant and may very well influence the dynamics of the positive energy states. The pulse itself is shown in the upper right corner

(22). Furthermore, both forms of the Hamiltonian have been implemented using each of the two ways of excluding negative energy states discussed in Sec. II A.

Figure 1 has several interesting features—the most interesting one being that *beyond* the dipole approximation the result coincides with the result *within* the dipole approximation when negative energy states of H_0 are excluded. This is in marked contrast to the nonrelativistic result which shows a substantial contribution from effects beyond the dipole approximation. When negative energy states are included, however, the converged result agrees very well with the nonrelativistic one. In other words, these states are absolutely necessary in order to account for nondipole effects. This conclusion is substantiated in Fig. 2. Here the total population of negative energy states, with respect to H_0, is plotted as a function of time. Note that this quantity is not physical in the sense that it depends on both gauge and rotation angle θ, which is $10°$ in this case. However, as this "population" is rather significant during the interaction, it still serves to illustrate that the result of a calculation may depend on whether they are included or not. Higher population of negative energy states is seen for stronger fields [2,5]. The distribution in negative energy states of H_0 is strongly concentrated just below the barrier at $-mc^2$, but at higher intensities a "tail" extending a few atomic units into the negative energy continuum is seen during interaction. To some extent this is a situation analogous to that for the inclusion of high partial waves, ℓ. Even when only modest ℓ values are found to be populated *after* the pulse, high ℓ values might be required *during* the pulse for a correct description of the dynamics, and the needed maximum ℓ is gauge dependent. Mathematically the substantial population of negative energy states can be understood from the fact that the interaction term is nondiagonal with respect to the upper and lower component of the wave function. A clear illustration of what happens is obtained if we consider the possibility to get an admixture of a virtual state m into the wave function describing an electron in state a. In second-order perturbation theory the state
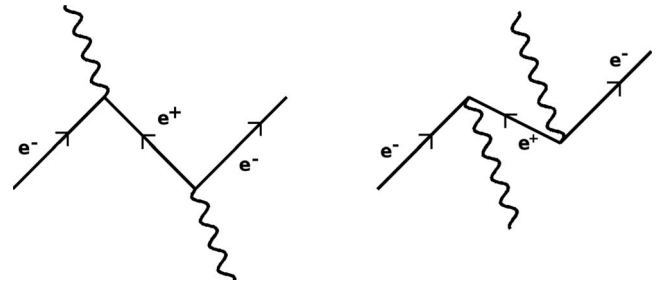

FIG. 3. Feynman diagrams describing electron-positron pair creation and the subsequent annihilation of the positron by another electron. In the left diagram the first photon (lower) is absorbed and the second is emitted. In the diagram to the right the situation is the opposite. If the photon energy would match the total energy of the two created particles, the left diagram would describe real pair creation. Far from resonance (i.e., when $\hbar\omega \ll 2mc^2$) the two diagrams might be of equal importance.

m will contribute to the energy of the electron in state a as

$$\Delta E \sim \sum_m \frac{\langle a|ec\boldsymbol{\alpha}\cdot\mathbf{A}|m\rangle\langle m|ec\boldsymbol{\alpha}\cdot\mathbf{A}|a\rangle}{E_a - E_m}. \tag{27}$$

If m is a positive energy state, the whole contribution is of order unity (in a.u.). The factor c^2 in the nominator compensates the radial integrals, which are small since the Dirac $\boldsymbol{\alpha}$ matrices mix the large and small components of the relativistic wave function. If m is a negative energy state, on the other hand, there are contributions to the radial integrals that are much larger, of the order unity. This is because the large and small components are found at opposite places in the eigenfunctions for positive and negative energy states. Now the energy denominator is of the order $2mc^2$, but this is compensated by the factor c^2 in the nominator and again the whole contribution is of the order unity. We see thus that when it comes to virtual states the role played by the negative energy states can be as important as that of the positive energy states. Note that although the expression in Eq. (27) is valid for both positive and negative energy states, they correspond to rather different time ordered Feynman diagrams. While the expression with a positive energy state, m, describes the fluctuation from a to m and back again, that with a negative energy state is describing the process when the excitation of an electron *from* the negative state m happens first. This creates a virtual electron-positron pair *in addition* to the already present electron; see Fig. 3. In a second step this electron annihilates the positron [24].

We emphasize that the contribution from virtual pairs depends on which Hamiltonian we use to distinguish between electrons and positrons. If we instead use the instantaneous Hamiltonian $H(t)$ for this purpose, the contributions from virtual electron-positron pairs are minimal when $\hbar\omega \ll 2mc^2$. A clear manifestation of this is that when the time-dependent Dirac equation is solved with the parameters given above, the population of negative energy states of $H(t)$ is zero to machine accuracy (if the time evolution is made with a small enough step) even if they are not actively removed. As men-
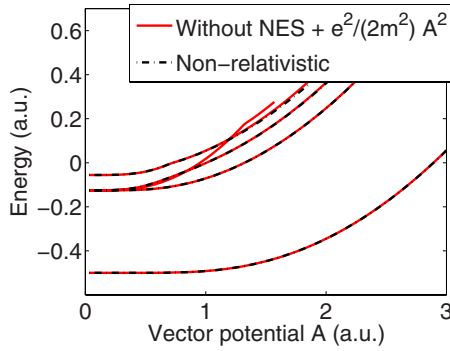
FIG. 4. (Color online) The lowest eigenenergies for a system "exposed to" a homogenous vector potential obtained in two ways. The dash-dotted curves are constructed from the lowest eigenenergies of the Schrödinger Hamiltonian including the diamagnetic term, cf. Eq. (4). The full curves are obtained through diagonalization of the Dirac Hamiltonian, Eq. (2), excluding states corresponding to negative energies ("NES") of the unperturbed Hamiltonian, and then adding the diamagnetic energy of the Schrödinger equation, $e^2/2m^2A^2$.

tioned, a similar conclusion was drawn by Boca and Florescu [5].

The importance of negative energy states, or virtual electron-positron pair creation, for certain processes has been observed before. In Ref. [9] Sakurai illustrates what happens very clearly. Thomson scattering, in which a highly energetic photon scatters off a free electron, is described to lowest order perturbation theory within the scope of both the Schrödinger equation and the Dirac equation. The nonrelativistic treatment describes the process as a first-order interaction through the diamagnetic term, whereas it is necessary to include second order in the relativistic description. Moreover, only when negative energy states are included in the sum over intermediate states is the cross section obtained from the Schrödinger equation reobtained. In other words, if negative energy states of the unperturbed system are left out altogether, the Dirac equation is not able to describe dynamics that arises from the diamagnetic term in the analogous Schrödinger representation (4). Since this term, $e^2/2mA^2$, only depends on time in the dipole approximation, it is at this level irrelevant for the dynamics. We also see numerically that inclusion of negative energy states is not crucial for the time-dependent Dirac equation within the dipole approximation. However, the diamagnetic term gives by far the largest contribution beyond the dipole approximation, and indeed, as is seen in Fig. 1, the relativistic nondipole results coincide with those from a nonrelativistic calculation only when negative energy states are included.

Figure 4 may serve to illustrate this phenomenon further. It shows the lower part of the eigenenergy spectrum for a hydrogen atom as a function of the magnitude of a homogenous external vector potential. These eigenenergies, which do not represent any physical quantity by themselves, are relevant for the time evolution of a system exposed to a time-dependent vector potential. The dash-dotted curves show the lowest eigenenergies of the Schrödinger Hamiltonian, cf. Eq. (4)—including the diamagnetic term. The full curves, on the other hand, are obtained from the eigener-

gies of the Dirac Hamiltonian, cf. Eq. (2), when diagonalized within a basis of eigenstates of H_0 corresponding to positive energies only—*plus* the nonrelativistic diamagnetic term, $e^2/2mA^2$. As the curves coincide only when this term is added, it is clear that the Dirac representation without negative energy states does *not* feature the analog of the diamagnetic term in the Schrödinger representation. In other words, phenomena that in the nonrelativistic representation involve this interaction term cannot be represented in a relativistic treatment *unless negative energy states of H_0 are included in the basis.*

It may seem odd that even though the results in Fig. 1 converge toward the same value in the dipole approximation, the convergence is quite different depending whether negative energy states of H_0 are included or not. I. e., for a calculation which is not convergent in $\ell_{\max}$, the truncation affects the two representations differently. This may be related to the fact that the correspondence with the diamagnetic term in the nonrelativistic case requires an adequate representation of the physical space. There is no obvious reason why the correspondence between the diamagnetic term and the inclusion of negative energy states should prevail in an incomplete description such as the one we have with truncation at a low $\ell_{\max}$. It is hard to draw a clear conclusion regarding in which case, with or without negative energy states, the convergence is fastest in the dipole approximation since the convergence pattern varies with field strength and frequency.

It is also worth noting that there is a practical aspect to the inclusion or truncation of negative energy states. When eigenstates with a very large energy magnitude are important for the time propagation, Eq. (25) indicates that a correspondingly smaller time step should be required. When negative energy states are included and important, one would suppose that the required time step would be $\Delta t \ll 1/2mc^2$. A full inclusion of negative energy states thus causes computational difficulties, at least if they are (virtually) populated. Even when they are *not* virtually populated with a short enough time step, a larger step size might result in spurious population. In this respect the definition of negative and positive energy states with respect to the instantaneous $H(t)$ has an advantage over that with respect to $H_0(t)$; with the former definition negative energy states can safely be neglected (as long as the intensities used are not enough for real pair production), while their inclusion is called for in the latter case. It is sometimes argued [3] that if the studied intensities are too low to allow for real pair production, negative energy states are not populated and a larger Δt is allowed. From the above considerations, this point of view is not completely justified.

As has been mentioned, the contribution from virtual electron-positron pairs is gauge dependent. It is thus interesting to discuss what the situation regarding negative energy states would be if the interaction with the electromagnetic field were studied in the length gauge. We follow here Ref. [25] and obtain the length gauge expression when H_D, Eq. (2), is transformed according to

$$UH_DU^\dagger + i\hbar\frac{\partial U}{\partial t}U^\dagger \qquad (28)$$

with

$$U = \exp\left(\frac{ie}{\hbar}\mathbf{A} \cdot \mathbf{r}\right). \tag{29}$$

The field interaction term in Eq. (2), $ec\boldsymbol{\alpha}\cdot\mathbf{A}$, is then replaced by

$$e\mathbf{r} \cdot \mathbf{E} + ec(\boldsymbol{\alpha} \cdot \mathbf{k})\left(\mathbf{r} \cdot \frac{d\mathbf{A}}{d\eta}\right). \tag{30}$$

Here an electric field term identical to the one in the nonrelativistic length gauge Hamiltonian appears, but there is now also an additional term. This term is proportional to the magnetic field and again we have a term nondiagonal with respect to the large and small component of the wave function. As was discussed above, important contributions beyond the dipole approximation arise when the electron is accelerated to high velocities by the electric field and then interacts with the magnetic field. In the length gauge such contributions would arise from the cross terms between the two operators in (30). Looking again at the matrix elements involved we have in analogy with Eq. (27)

$$\Delta E \sim \sum_m \frac{\langle a|e\mathbf{r} \cdot \mathbf{E}|m\rangle\langle m|ec(\boldsymbol{\alpha} \cdot \mathbf{k})\left(\mathbf{r} \cdot \frac{\partial\mathbf{A}}{\partial\eta}\right)|a\rangle}{E_a - E_m}. \tag{31}$$

It is easy to see that for positive energy states, m, the first matrix element is large, but the second is suppressed. For negative energy states, m, the situation is the opposite; it is the first matrix element that is suppressed and the second that is large. However, the energy denominator is in the second case large, $\sim 2mc^2$, and the whole contribution is thus a factor α^2 (with α being the fine structure constant) smaller than when m is a positive energy state. Thus, negative energy states are here not contributing in leading order but in relative order α^2, which is the same order as relativistic effects in general.

It might be possible to push the contributions from virtual electron-positron pairs even further away. Consider the alternative transformation

$$U = \exp\left[\frac{1}{2}(\beta mc^2)^{-1}(ec\boldsymbol{\alpha} \cdot \mathbf{A})\right] = \exp\left(\frac{e}{2mc}\beta\boldsymbol{\alpha} \cdot \mathbf{A}\right), \tag{32}$$

where the exponent is half the ratio of the interaction energy over the mass energy. The result of this transformation on the wave function cannot be written in closed form, but expanding it in terms of the aforementioned ratio we find in leading order that the interaction may be written

$$H' = \frac{e}{m}\beta\mathbf{A} \cdot \mathbf{p} + \frac{e^2}{2m}\beta\mathbf{A}^2 + \frac{e\hbar}{2m}\beta\boldsymbol{\sigma} \cdot \mathbf{B} + O\left(\beta\frac{ec\boldsymbol{\alpha} \cdot \mathbf{A}}{mc^2}\right). \tag{33}$$

Here all the nonrelativistic velocity gauge operators, including the diamagnetic term, reappear although still in the framework of the four-component Dirac equation. Also the spin-dependent interaction is here easily recognized. Note that the first three terms are all diagonal with respect to the small and large components of the wave function and we

expect very small contributions from virtual electron-positron pairs (negative energy states). Again this underlines the close connection between these contributions and the diamagnetic term.

B. Relativistic effects for systems of high nuclear charges

Relativistic effects arise when the atomic system is exposed to external fields which drives the electron up to relativistic velocities. In addition, highly charged ions are "intrinsically relativistic" in the sense that the Coulomb potential alone causes the energy level of the atom to deviate strongly from the Bohr formula. When such a system is exposed to strong external fields, a relativistic treatment should be necessary in order to describe the dynamics.

When we study the dynamics for hydrogenlike systems of different nuclear charges Z, we may scale the field parameters such that the dynamics becomes analogous for every nuclear charge. As is well known, the time-dependent Schrödinger equation, for a time independent Hamiltonian, remains the same for any Z if the time t and position $\mathbf{r}$ are substituted by $\tilde{t} \equiv Z^2 t$ and $\tilde{\mathbf{r}} \equiv Z\mathbf{r}$, respectively. Furthermore, the addition of a time-dependent perturbation within the dipole approximation preserves this Z dependence if the electric field strength, E_0, and the central frequency of the field, ω, are also scaled. Specifically, they should be substituted by

$$\tilde{E}_0 = E_0/Z^3,$$

$$\tilde{\omega} = \omega/Z^2, \tag{34}$$

respectively, cf. [1]. The Dirac equation reproduces the scaling of the Schrödinger equation only in the nonrelativistic limit. Hence, any deviation from properly scaled predictions from a solution of the time-dependent Schrödinger equation in the dipole approximation for, e.g., hydrogen is either a relativistic effect or a magnetic one.

Figure 5 shows the ionization rate for various hydrogenlike ions exposed to monochromatic fields with $\omega = 1.0Z^2$ a.u. (i.e., with $\tilde{\omega} = 1.0$ a.u.). The nuclear charges follow the noble gas sequence, except for $Z = 1$ and 70. Of course, when $\tilde{E}_0$ and $\tilde{\omega}$ of Eq. (34) are held fixed, the true field parameters become rather unrealistic for the higher nuclear charges. However, we still find these calculations interesting as they say something about to what extent relativistic effects become important as the nuclear charge increases.

We will start by discussing the results obtained within the dipole approximation. These correspond to the full and the dashed curves in Fig. 5. Here the rates are found via an exponential fit to $\Sigma_n|c_n|^2$ of Eq. (23). Note that due to the complex rotation, this sum is for the most part a decreasing function in time. For these calculations the negative energy states of H_0 have been removed in the relativistic version (which does not affect the result within the dipole approximation as discussed above), and hence the dynamics can be resolved by the Runge-Kutta method. The rotation angle θ is here 15°. This method of obtaining ionization rates is
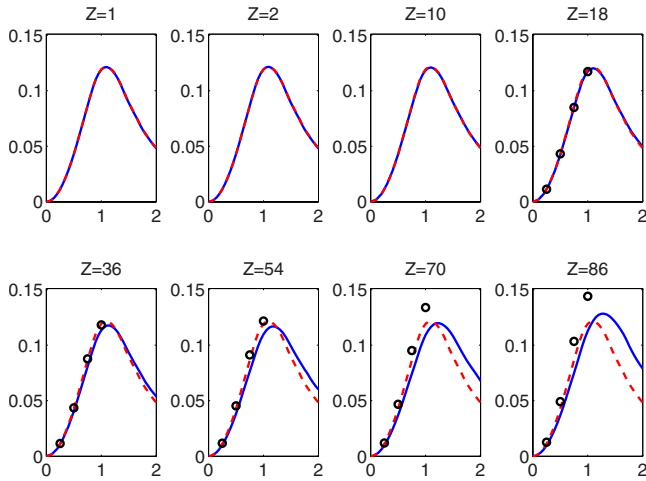
FIG. 5. (Color online) The ionization rate of hydrogenlike systems exposed to a monochromatic laser of photon energy $\hbar\omega = 1.0Z^2$ a.u., where Z is the nuclear charge, as functions of the amplitude E_0 of the electric field. The field on the x axis is given in units of Z^3 a.u., i.e., the x axis corresponds to $\widetilde{E}_0$ of Eq. (34), and the rates on the y axis are given in units of Z^2 a.u.. The full (blue) curves are the results of relativistic calculations, whereas the dashed (red) curves stem from nonrelativistic calculations—both within the dipole approximation. The black circles are the results from relativistic calculations beyond the dipole approximation.

described in detail in Ref. [19]. The pulse has a constant amplitude between a two-cycle ramping on and off.

It is seen that the system features stabilization; the ionization rate is *not* monotonously increasing with the amplitude of the electromagnetic field. A clear and pronounced stabilization peak is seen near $\widetilde{E}_0 = 1.0$ a.u. for all nuclear charges. Furthermore, within the dipole approximation, we do not see any significant differences between relativistic and nonrelativistic calculations until we reach $Z = 36$. Beyond this nuclear charge, however, the stabilization peaks for the relativistic calculations are increasingly shifted outwards relative to $\widetilde{E}_0$. This may be understood in the context of high frequency Floquet theory [26]. According to this formalism, a sufficient criterion for stabilization may be written as

$$\hbar\omega \geqslant |W(\alpha_0)|, \qquad (35)$$

where the parameter $\alpha_0 \equiv eE_0/m\omega^2$ is the amplitude of the quiver motion of a free classical electron. W is the effective (or dressed) ground-state energy in the high frequency limit. It is shown in Ref. [26] to increase from the true ground-state energy toward zero as α_0 increases. Since the relativistic ground-state energy is lower than the nonrelativistic one (presumably also its effective ground-state energy W for all α_0), a higher value of the electric-field strength is necessary to satisfy condition (35) than in the nonrelativistic case, which explains the observed shift.

When it comes to the magnitude of the ionization rates, we see that the ones obtained via the Dirac equation are lower than the ones obtained with the Schrödinger equation for $Z = 36$ and 54, whereas they are more or less equal for $Z = 70$, and for $Z = 86$, the relativistic ionization rate reaches a

higher value than the nonrelativistic one. The latter situation seems to be more easily understood since absorption of one photon of energy $\hbar\omega$ brings the photoelectron closer to the threshold, where the density of states is high, in the relativistic case. However, for slightly lower nuclear charges, this effect is seen to be dominated by some other effect—possibly one related to the increased inertia of the relativistic electron induced by the external field.

Although the dynamics in the hydrogen case ($Z = 1$) is well described within the dipole approximation, cf. [27], it is expected that this approximation will eventually break down as Z increases. This can be seen from classical considerations; the translation of the electron due to the magnetic field per optical cycle should be of the order $e^2E_0^2/cm^2\omega^3 = e^2\widetilde{E}_0^2/cm^2\widetilde{\omega}^3$. In other words, this translation is unaffected by Z when $\widetilde{\omega}$ and $\widetilde{E}_0$ are held fixed. However, the extension of the initial state and the wavelength of the external field is shortened by a factor Z^{-1} and Z^{-2}, respectively, and therefore the relative importance of the magnetic translation increases.

The results from solving the Dirac equation beyond the dipole approximation are indicated in Fig. 5 by black circles. Indeed it is clearly seen that the ionization rates differ from the ones predicted in the dipole approximation for higher nuclear charges. As mentioned, since the ionization rate is a quantity extracted during the interaction with the pulse at maximum, it cannot be sensitive to whether the spatial dependence of the envelope is included or not. Hence, the interaction Hamiltonian of Eq. (21) should be adequate. For these calculations the method corresponding to Eq. (26) has been used (including negative energy states of H_0). The rotation angle is here 2°. As these calculations are considerably more complicated than the ones performed in the dipole approximation, precise conclusions about the ionization dynamics with the full interaction are hard to draw at this point. However, it is clearly seen that inclusion of the magnetic field increases the overall ionization rate.

It should be noted that for the higher nuclear charges, and correspondingly higher photon energies, production of real electron-positron pairs, which is not accounted for by the present method, becomes more and more plausible and may possibly take place for the most intense fields considered here. For instance, an energy of $4.6\hbar\omega$, i.e., only five photons, is necessary to create a real electron-positron pair for $Z = 86$.

V. CONCLUSIONS

We have demonstrated that in order to describe dynamics of an atomic system exposed to strong external light sources using the time-dependent Dirac equation in the velocity gauge, the negative energy states of the unperturbed Hamiltonian H_0 *must* be included in the representation. If these states are excluded, the time-dependent Dirac equation is unable to give the correct results—even in the nonrelativistic limit. We argued that the "filled sea" of negative energy states should be associated with the time-dependent Hamiltonian at each time—not with the unperturbed one (H_0).

It was seen that the dynamics arising from the negative energy states of H_0 is related to the diamagnetic part of the

corresponding nonrelativistic Hamiltonian. Hence, exclusion of negative energy states of H_0 still gives correct results within the dipole approximation.

The situation for other gauges was briefly discussed. It seems that creation of virtual electron-positron pairs is of less importance in certain alternative descriptions of the interaction, e.g., in length gauge.

Finally, we used the relativistic formalism to study the ionization rates for various hydrogenlike systems, with the external field scaled with the nuclear charge to give identical rates in the nonrelativistic limit in the dipole approximation.

Relativistic effects were seen for higher charges. These were explained in terms of relativistic shifts in the effective binding energy. Magnetic effects were seen to contribute to enhance the ionization rate.

ACKNOWLEDGMENTS

[1] L. N. Gaier and C. H. Keitel, Phys. Rev. A **65**, 023406 (2002).

[2] N. J. Kylstra, A. M. Ermolaev, and C. J. Joachain, J. Phys. B **30**, L449 (1997).

[3] U. W. Rathe, C. H. Keitel, M. Protopapas, and P. L. Knight, J. Phys. B **30**, L531 (1997).

[4] G. Mocken and C. H. Keitel, J. Phys. B **37**, L275 (2004).

[5] M. Boca and V. Florescu, Eur. Phys. J. D **46**, 15 (2008).

[6] Y. I. Salamin, S. Hu, K. Z. Hatsagortsyan, and C. H. Keitel, Phys. Rep. **427**, 41 (2006).

[7] W. H. Furry, Phys. Rev. **81**, 115 (1951).

[8] P. A. M. Dirac, Proc. R. Soc. London **126**, 360 (1930).

[9] J. J. Sakurai, *Advanced Quantum Mechanics* (Addison-Wesley, Reading, MA, 1967).

[10] A. Bugacov, M. Pont, and R. Shakeshaft, Phys. Rev. A **48**, R4027 (1993).

[11] J. R. Vázquez de Aldana, N. J. Kylstra, L. Roso, P. L. Knight, A. Patel, and R. A. Worthington, Phys. Rev. A **64**, 013411 (2001).

[12] M. Førre, Phys. Rev. A **74**, 065401 (2006).

[13] L. L. Foldy and S. A. Wouthuysen, Phys. Rev. **78**, 29 (1950).

[14] D. V. Fursa and I. Bray, Phys. Rev. Lett. **100**, 113201 (2008).

[15] J.-L. Heully, I. Lindgren, E. Lindroth, and A.-M. Mårtensson-Pendrill, Phys. Rev. A **33**, 4426 (1986).

[16] J. Schwinger, Phys. Rev. **82**, 664 (1951).

[17] S. Salomonson and P. Öster, Phys. Rev. A **40**, 5548 (1989).

[18] M. Tokman, N. Eklöw, P. Glans, E. Lindroth, R. Schuch, G. Gwinner, D. Schwalm, A. Wolf, A. Hoffknecht, A. Müller, and S. Schippers, Phys. Rev. A **66**, 012703 (2002).

[19] J. Bengtsson, E. Lindroth, and S. Selstø, Phys. Rev. A **78**, 032502 (2008).

[20] H. A. Antosiewicz, in *Handbook of Mathematical Functions*, 4th ed., edited by M. Abramowitz and I. A. Stegun (National Bureau of Standards, Washington, DC, 1964), p. 437.

[21] I. J. Thompson and A. R. Barnett, J. Comput. Phys. **64**, 490 (1986).

[22] K. J. Meharg, J. S. Parker, and K. T. Taylor, J. Phys. B **38**, 237 (2005).

[23] F. He, C. Ruiz, and A. Becker, Phys. Rev. A **75**, 053407 (2007).

[24] The attentive reader might remark that this is a Pauli principle violating process; since there is already an electron in *a* the electron in the virtual electron-positron pair can go anywhere but to *a*. However, this Pauli violating diagram is canceling another Pauli violating diagram that is implicitly included when the vacuum level is redefined. This has been carefully examined by Furry [7].

[25] S. Selstø and M. Førre, Phys. Rev. A **76**, 023427 (2007).

[26] M. Gavrila, J. Phys. B **35**, R147 (2002).

[27] O. Latinne, C. J. Joachain, and M. Dörr, Europhys. Lett. **26**, 333 (1994).